Supporting Information

**A Site-Isolated Iridium Diethylene Complex Supported on Highly
Dealuminated Y Zeolite: Synthesis and Characterization**

Alper Uzun, Vinesh A. Bhirud, Philip W. Kletnieks,
James F. Haw, and Bruce C. Gates*

Department of Chemical Engineering and Materials Science
University of California, Davis, CA 95616
and
Department of Chemistry
University of Southern California, Los Angeles, CA 90086

TABLE SI-1. EXAFS Results: Goodness of Fit Parameter and Variance between Data and Fit

Sample name	Goodness of fit[a]	k^0-weighted variance[b] (%)	k^2-weighted variance[b] (%)	Variance in R space,[b,c] with a k^1 weighting (%) ($\Delta R = 1.0–4.0$ Å) Imaginary	Absolute
As-prepared sample ($\Delta k = 2.9–15$ Å^{-1})	8.9	4.7	5	0.9	0.1
Sample after CO treatment ($\Delta k = 3.1–13.8$ Å^{-1})	3.5	4.2	8.0	1.7	0.9
Sample after ethylene hydrogenation for 10 h in a once-through flow reactor ($\Delta k = 2.9–10.1$ Å^{-1})	2.5	3.4	14.2	1.5	0.8

[a] Goodness of fit values are calculated by XDAP as follows:

$$goodness\ of\ fit = \frac{v}{NPTS(v - N_{free})} \sum_{i=1}^{NPTS} \left(\frac{\chi_{exp,i} - \chi_{model,i}}{\sigma_{exp,i}} \right)^2$$

[b] Variance between the k-weighted Fourier transform of the data and the fit over the fitting range (1.0–4.0 Å) was calculated by XDAP as follows:

$$k^n\ variance = \frac{\int [k^n(\chi_{model}(k) - \chi_{exp}(k))]^2\ dk}{\int [k^n \chi_{exp}(k)]^2\ dk} \times 100$$

[c] Variance in R space is calculated by XDAP as follows:

$$k^n\ variance = \frac{\int [k^n(FT_{model}(R) - FT_{exp}(R))]^2\ dR}{\int [k^n FT_{exp}(R)]^2\ dR} \times 100$$
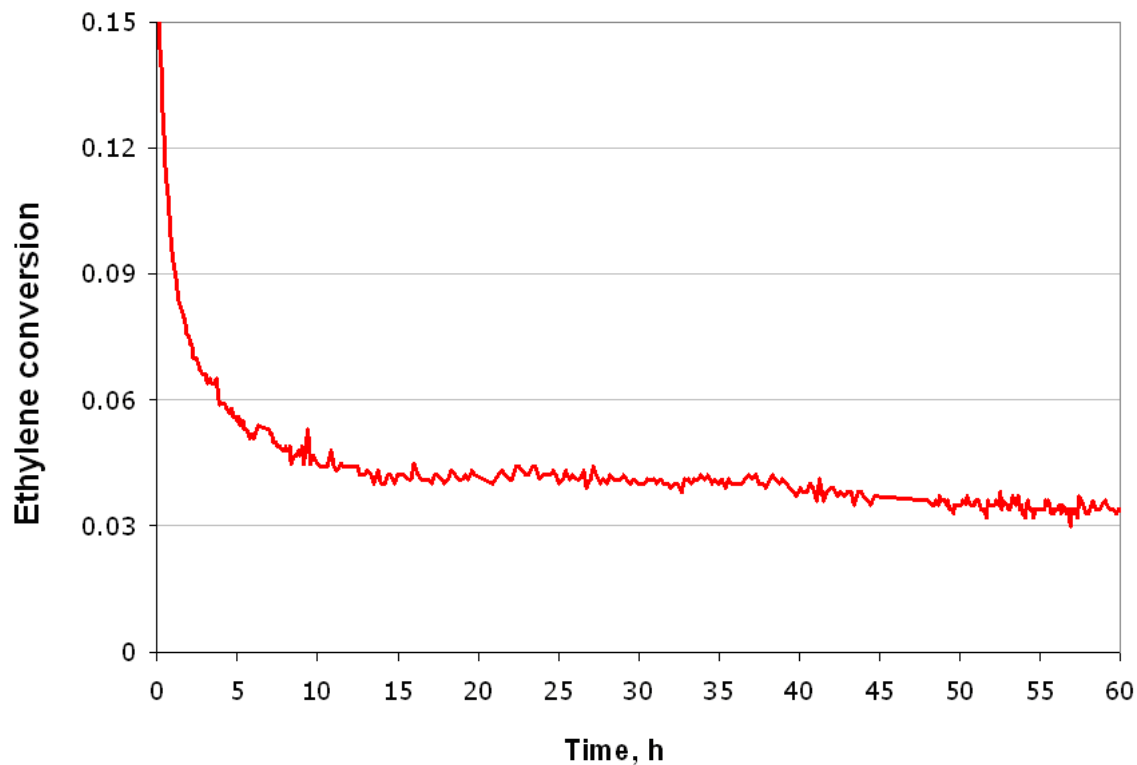
Figure SI-1. Ethylene hydrogenation catalyzed by sample formed from chemisorption of Ir(C$_2$H$_4$)$_2$(acac) on DAY zeolite: conversion of ethylene versus time on stream in a flow reactor with a total flow rate of 100 mL/min, in the presence of 40 mbar of ethylene and 40 mbar of H$_2$ (in a balance of He) at 294 K and atmospheric pressure with 30 mg of catalyst.
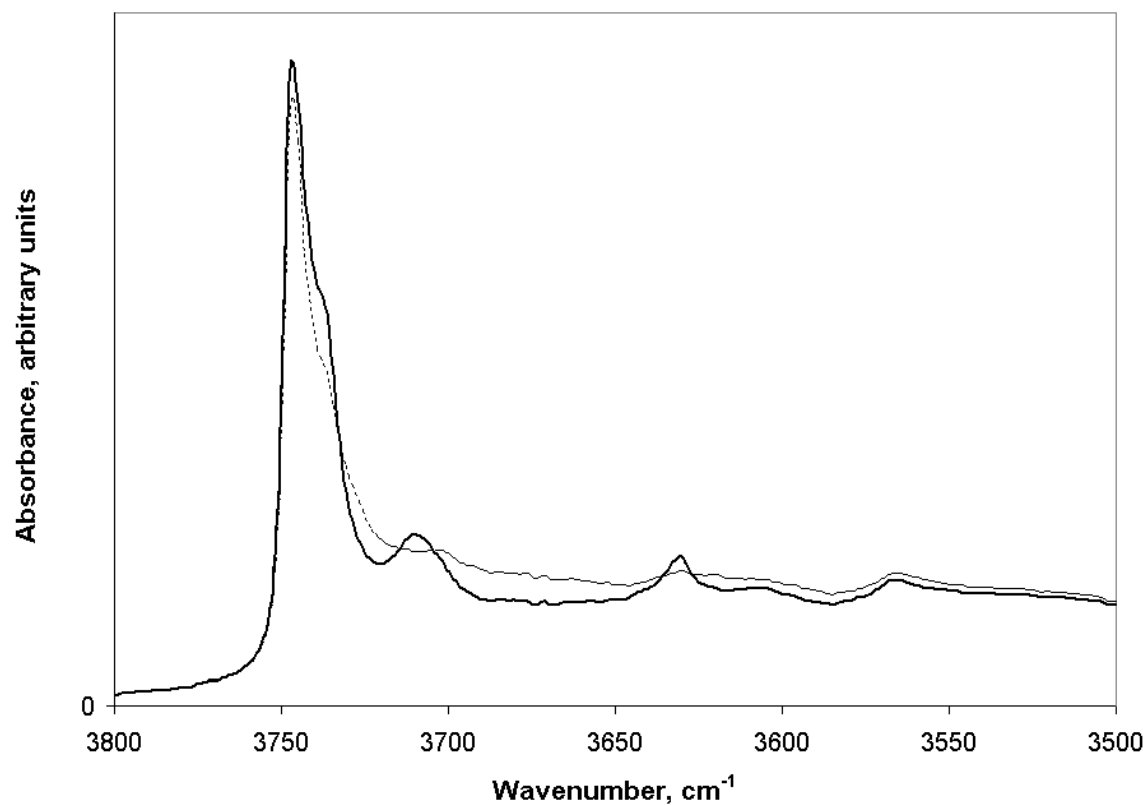
Figure SI-2. IR spectra in the ν_{OH} region during treatment in flowing helium of the zeolite-supported iridium-ethylene complex; dotted line: before start of helium flow; solid line: after 20 min of continuous helium flow.
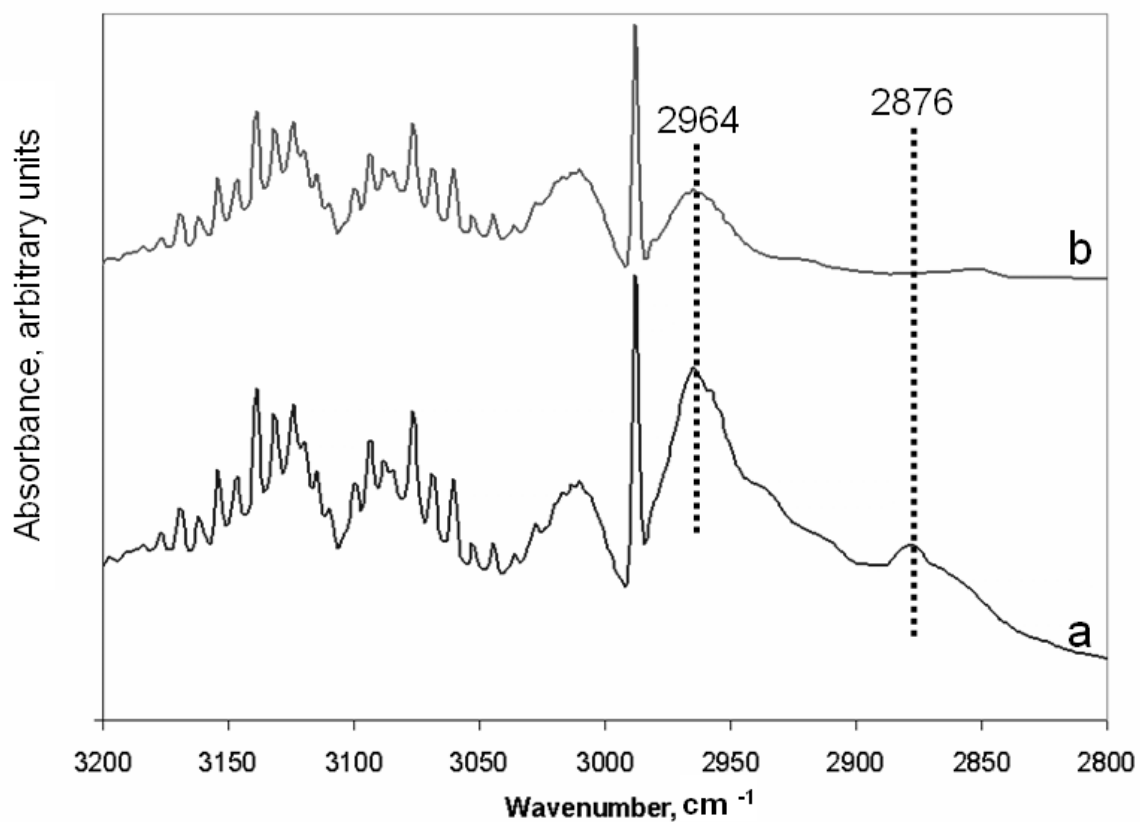
Figure SI-3. Difference IR spectra in the υ_{CH} region during treatment in C_2H_4 of the zeolite-supported iridium-ethylene complex; bands at 2964 and 2876 cm^{-1} suggested to represent ethyl; (a) difference spectrum at the end of C_2H_4 flow; (b) IR spectrum of gas-phase ethylene.
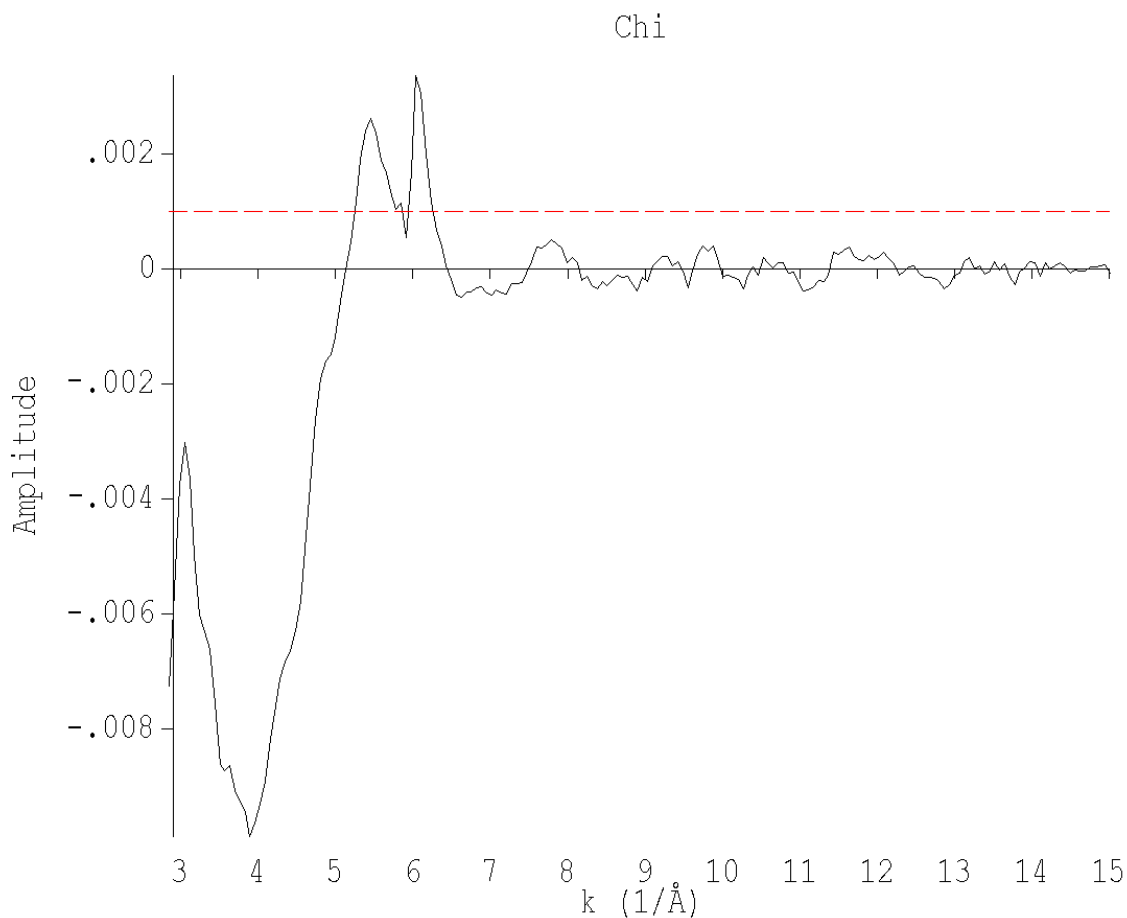
Figure SI-4. Standard deviations in the EXAFS function and the residuals of the model fit from the data for the supported sample formed by the reaction of $Ir(C_2H_4)_2(acac)$ with dealuminated Y zeolite. Solid line, residuals remaining when the sum of the calculated contributions (to the chi file) were subtracted from the raw data; dotted line, averaged standard deviation for the raw data (compare the scale of the vertical axis with that of Figure 1A in the text).
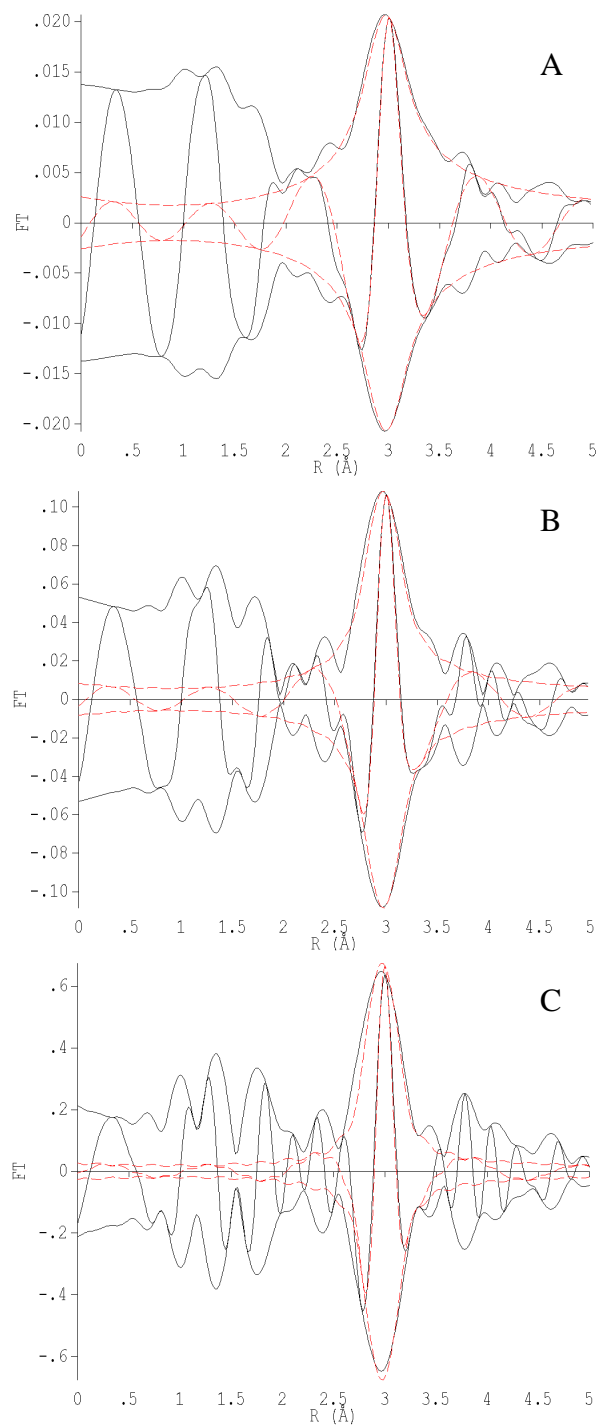
Figure SI-5. Imaginary part and magnitude of phase- and amplitude-corrected Fourier transform (A, unweighted; B, k^1-weighted; and C, k^2-weighted, and $\Delta k = 2.9$–15 Å^{-1}) of raw data minus calculated Ir–O, Ir–C, and Ir–O$_l$ contributions (solid line) and calculated Ir-Al contribution (dotted line) characterizing the sample formed from Ir(C$_2$H$_4$)$_2$(acac) and DAY zeolite.
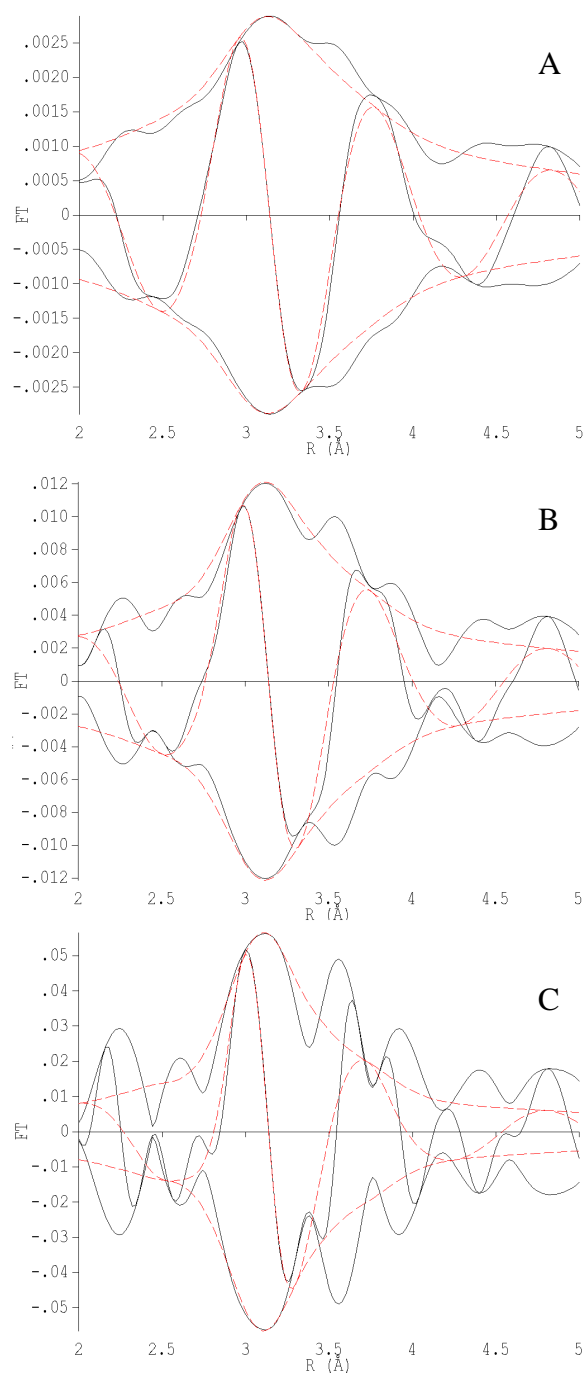
Figure SI-6. Imaginary part and magnitude of uncorrected Fourier transform (A, unweighted; B, k^1-weighted; and C, k^2-weighted, and $\Delta k = 2.9$–15 $\mathring{A}^{-1}$) of raw data minus calculated Ir–O, Ir–C, and Ir–Al contributions (solid line) and calculated Ir–O$_l$ contribution (dotted line) characterizing the sample formed from Ir(C$_2$H$_4$)$_2$(acac) and DAY zeolite. This is not a bonding Ir–O distance.
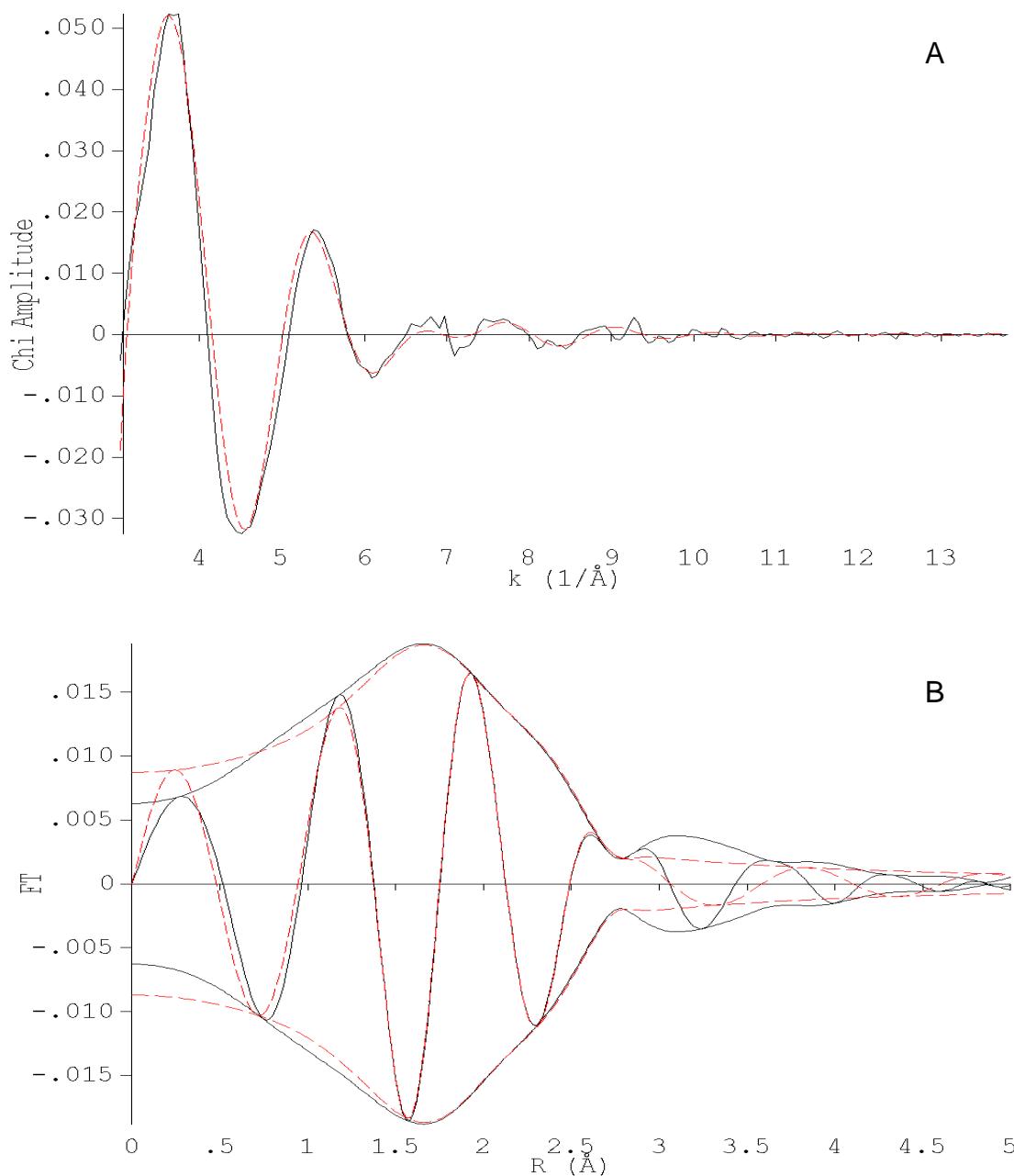
Figure SI-7. Results of EXAFS analysis characterizing the sample after 20 min of treatment in flowing CO at 1 atm and room temperature. (A) EXAFS function, χ (solid line), and calculated contribution (dotted line). (B) Imaginary part and magnitude of the Fourier transform of data (solid lines), and calculated (dotted lines) (unweighted, $\Delta k = 3.1–13.8$ Å^{-1}).
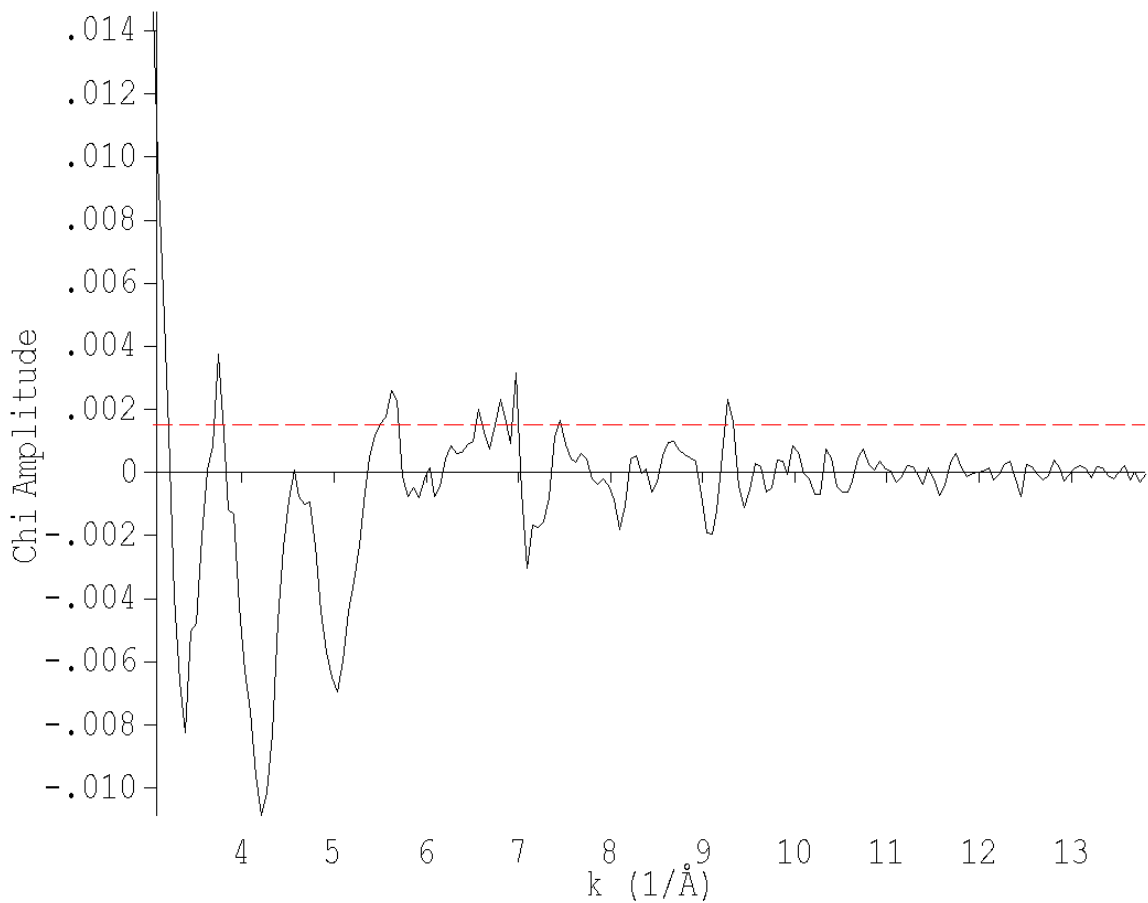
Figure SI-8. Standard deviations in the EXAFS function and the residuals of the model fit from the data for the sample obtained after 20 min of treatment in CO of the supported sample. Solid line, residuals remaining when the sum of the calculated contributions (to the chi file) are subtracted from the raw data; dotted line, averaged standard deviation for the raw data (compare the scale of the vertical axis with that of Figure SI-7).
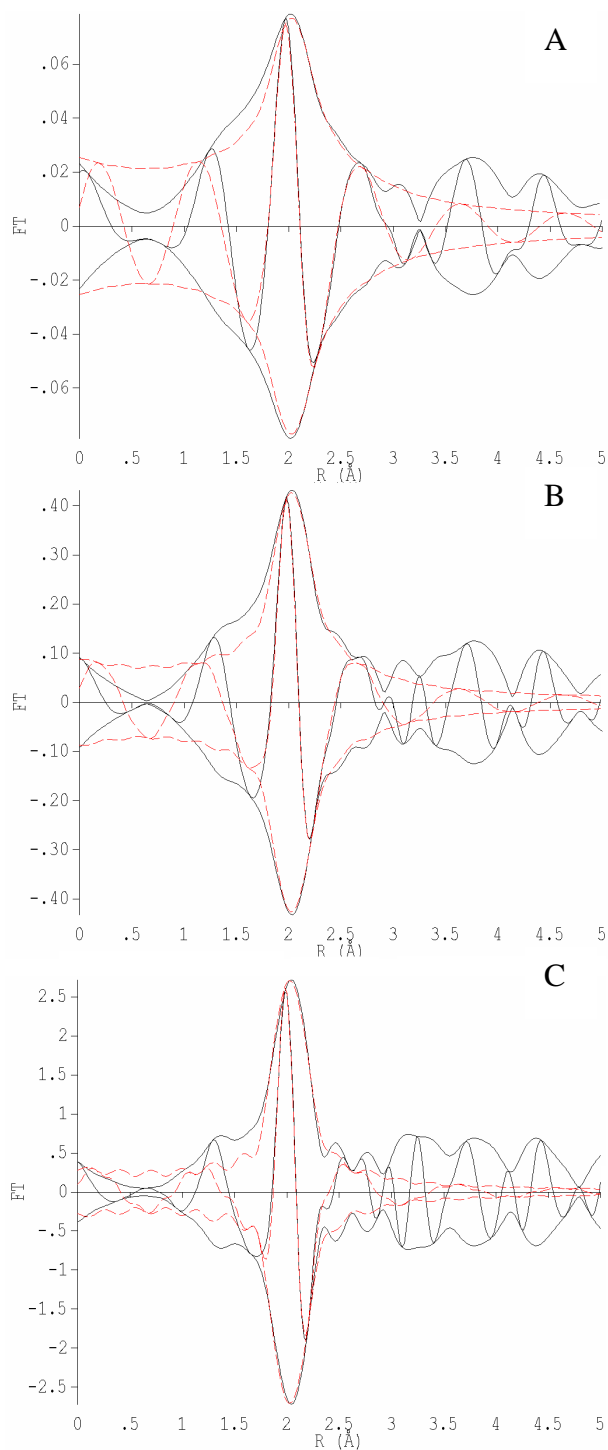
Figure SI-9. Imaginary part and magnitude of phase- and amplitude-corrected Fourier transform (A, unweighted; B, k^1-weighted; and C, k^2-weighted, and $\Delta k = 3.1-13.8$ Å^{-1}) of raw data minus calculated Ir−O, Ir−Al, and Ir−O* contributions (solid line) and calculated Ir−C contribution (dotted line) characterizing the sample obtained after 20 min of treatment in flowing CO of the supported sample.
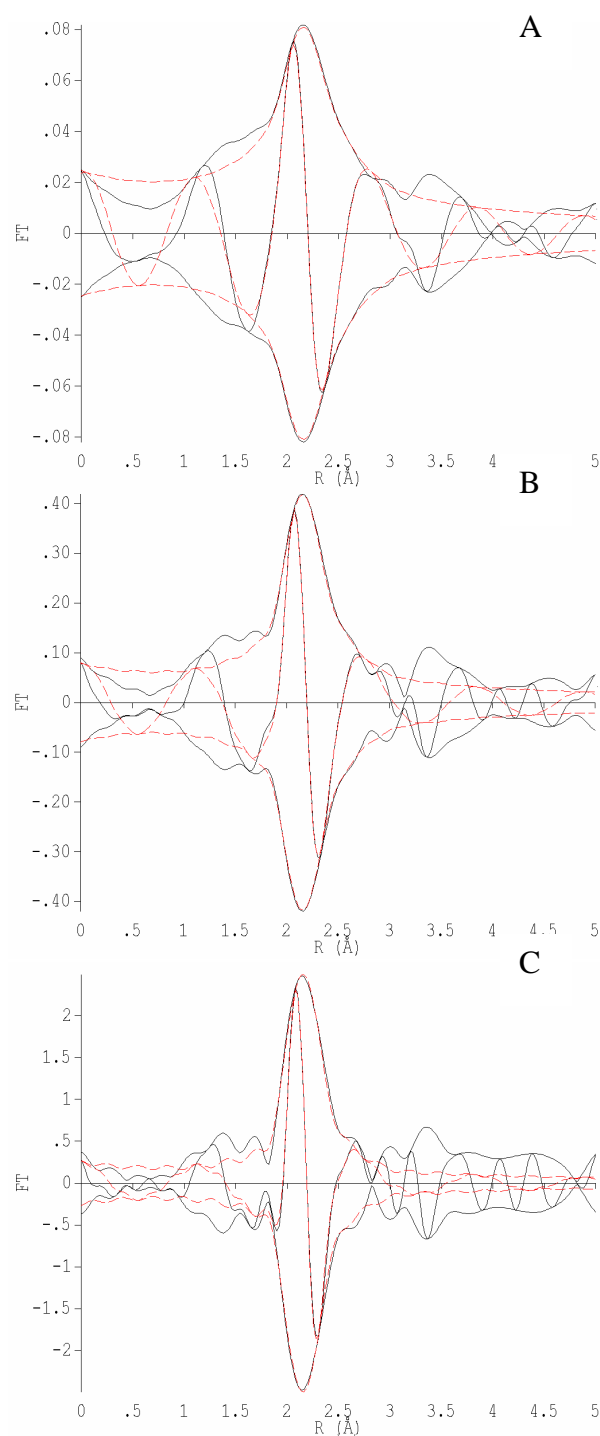
Figure SI-10. Imaginary part and magnitude of phase- and amplitude-corrected Fourier transform (A, unweighted; B, k^1-weighted; and C, k^2-weighted, and $\Delta k = 3.1–13.8$ Å^{-1}) of raw data minus calculated Ir–C, Ir–Al, and Ir–O* contributions (solid line) and calculated Ir-O contribution (dotted line) characterizing the sample obtained after 20 min of treatment in flowing CO of the supported sample. This is a bonding Ir–O contribution.
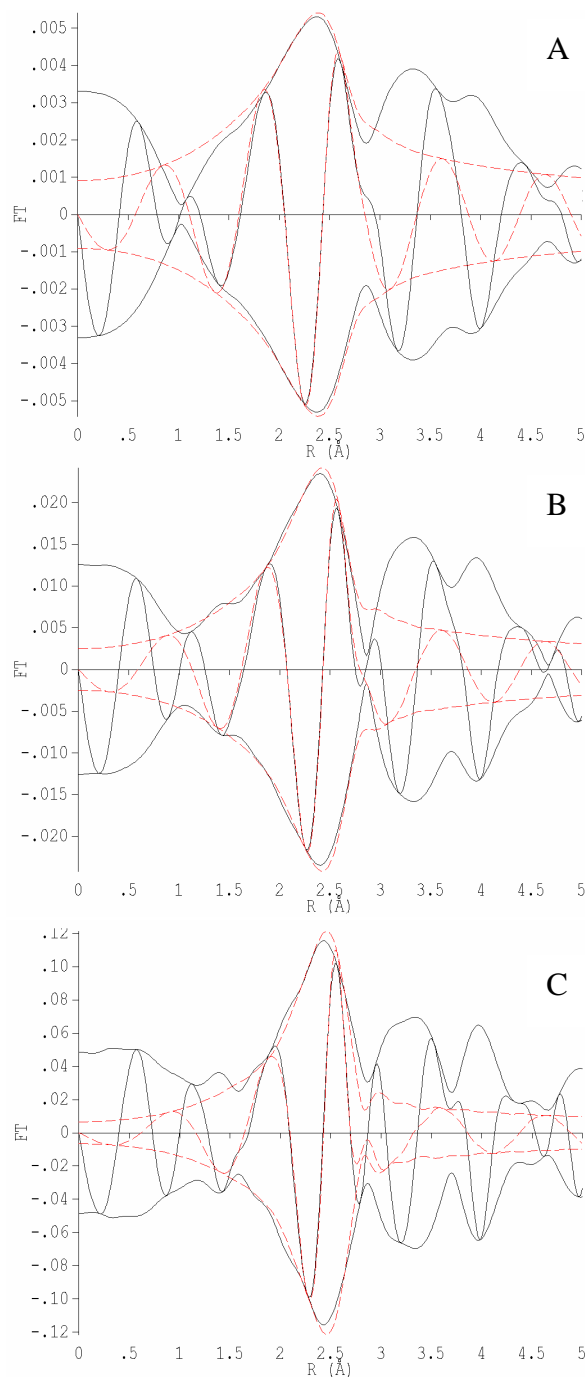
Figure SI-11. Imaginary part and magnitude of uncorrected Fourier transform (A, unweighted; B, k^1-weighted; and C, k^2-weighted, and $\Delta k = 3.1-13.8$ Å^{-1}) of raw data minus calculated Ir-C, Ir-O and Ir-Al contributions (solid line) and calculated contributions (dotted lines) of the individual Ir−O* (multiple scattering oxygen atom from the carbonyl ligand) contribution characterizing the sample obtained after 20 min treatment in flowing CO of the supported sample.
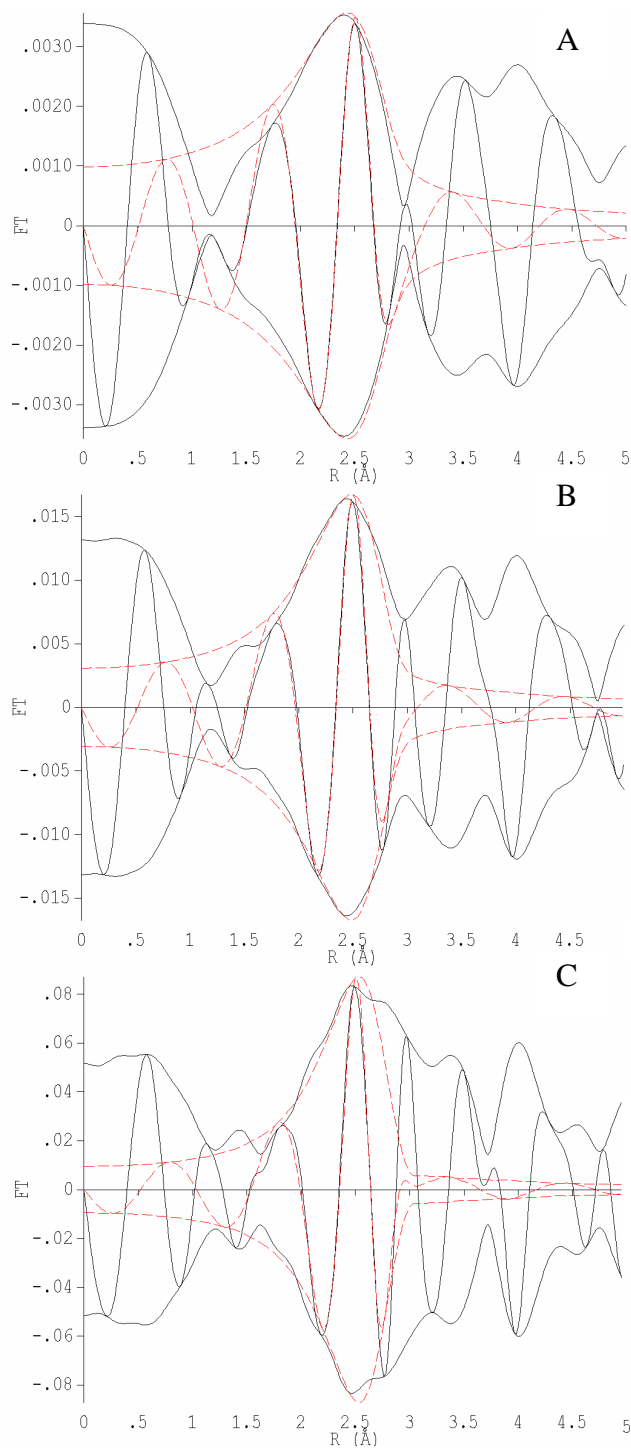
Figure SI-12. Imaginary part and magnitude of uncorrected Fourier transform (A, unweighted; B, k^1-weighted; and C, k^2-weighted, and $\Delta k = 3.1–13.8$ Å^{-1}) of raw data minus calculated Ir-C, Ir-O and Ir-O* contributions (solid line) and calculated Ir-Al contribution (dotted line) characterizing the sample obtained after 20 min of treatment in flowing CO of the supported sample.
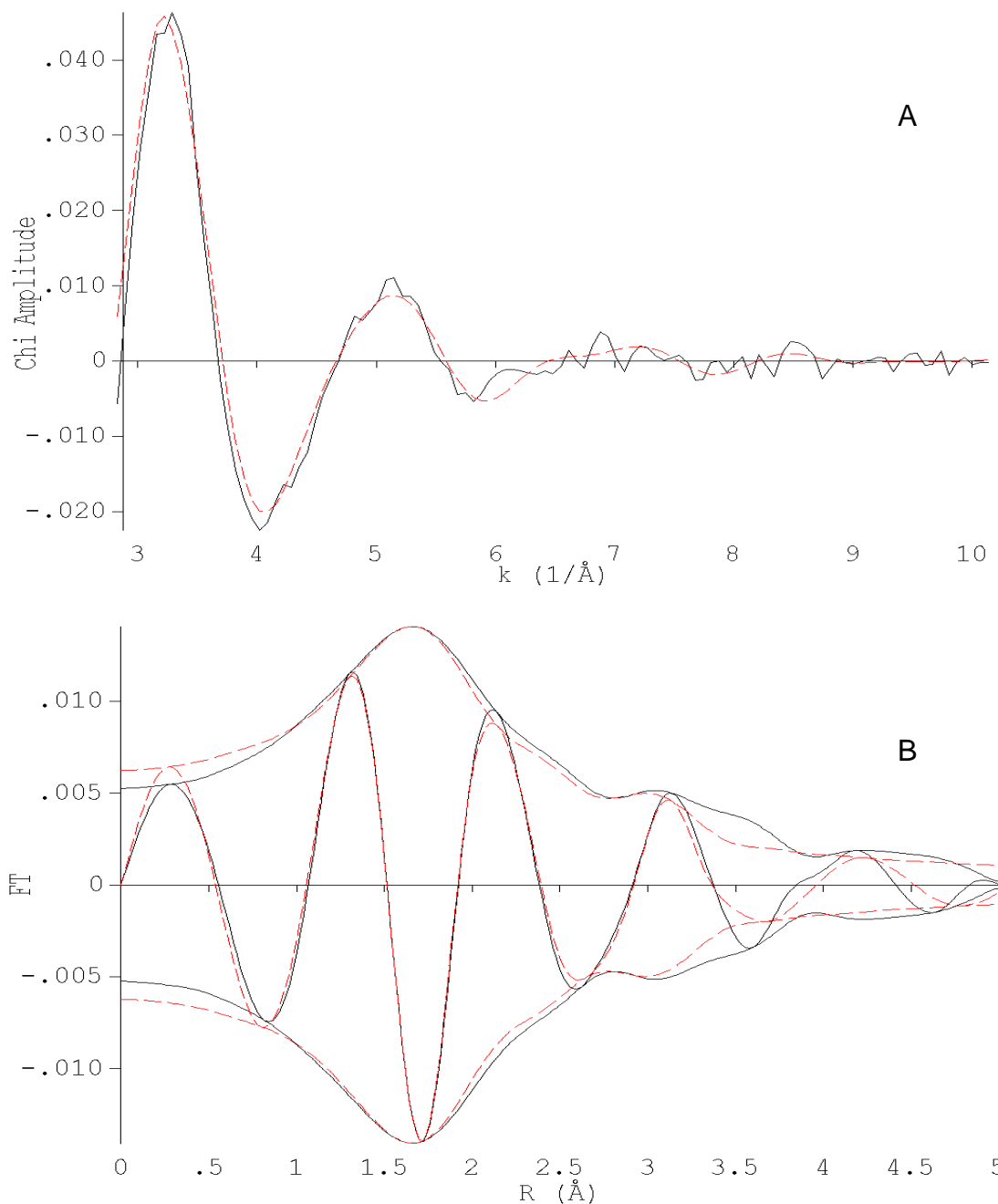
Figure SI-13. Results of EXAFS analysis characterizing the sample after 10 h of ethylene hydrogenation reaction under conditions stated in the text. (A) EXAFS function, χ (solid line), and calculated contribution (dotted line). (B) Imaginary part and magnitude of the Fourier transform of data (solid lines), and calculated (dotted lines) (unweighted, $\Delta k = 2.9–10.1$ Å^{-1}).
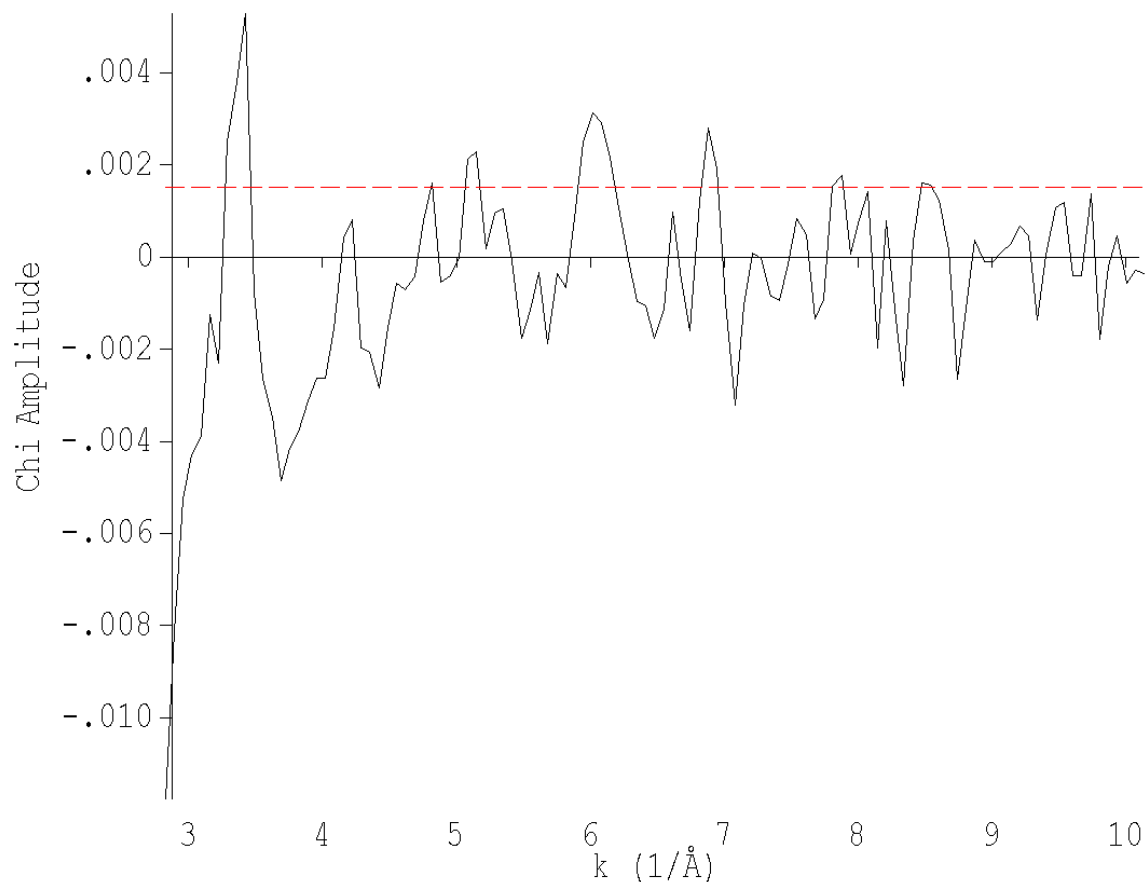
Figure SI-14. Standard deviations in the EXAFS function and the residuals of the model fit from the data for sample after 10 h of ethylene hydrogenation reaction under conditions stated in the text. Solid line, residuals remaining when the sum of the calculated contributions (to the chi file) were subtracted from the raw data; dotted line, averaged standard deviation characterizing the raw data (compare the scale of the vertical axis with that of Figure SI-13).
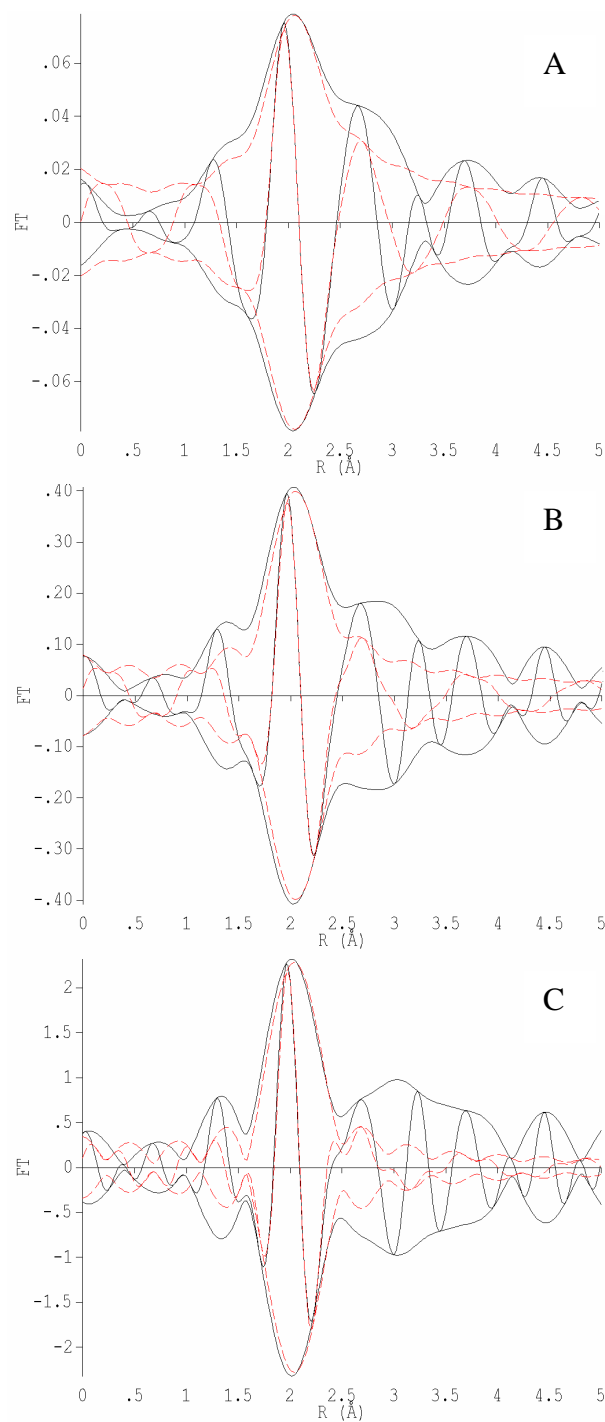
Figure SI-15. Imaginary part and magnitude of phase- and amplitude-corrected Fourier transform (A, unweighted; B, k^1-weighted; and C, k^2-weighted, and $\Delta k = 2.9$–10.1 Å^{-1}) of raw data minus calculated Ir–O, and Ir–Si contributions (solid line) and calculated Ir-C contribution (dotted line) characterizing the sample after 10 h of ethylene hydrogenation reaction under conditions stated in the text.

Figure SI-16. Imaginary part and magnitude of phase- and amplitude-corrected Fourier transform (A, unweighted; B, k^1-weighted; and C, k^2-weighted, and $\Delta k = 2.9–10.1$ Å^{-1}) of raw data minus calculated Ir−C, and Ir−Si contributions (solid line) and calculated Ir-O contribution (dotted line) characterizing the sample after 10 h of ethylene hydrogenation reaction under conditions stated in the text.
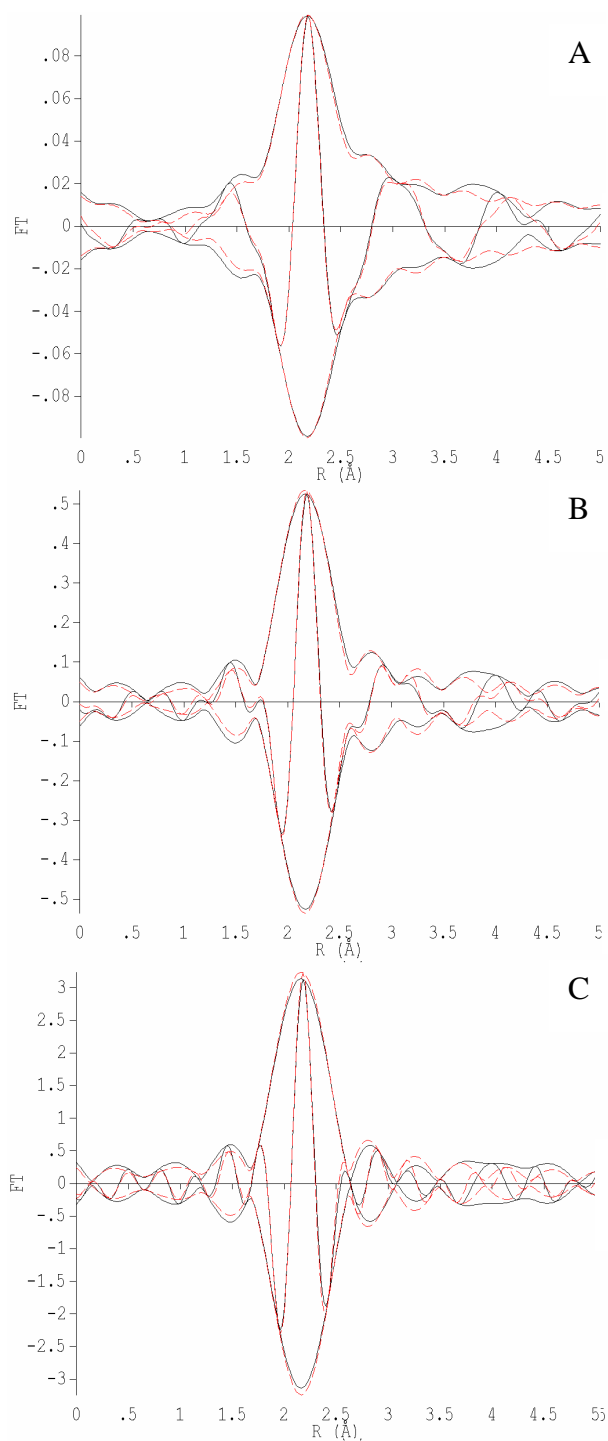
Figure SI-17. Imaginary part and magnitude of uncorrected Fourier transform (A, unweighted; B, k^1-weighted; and C, k^2-weighted, and $\Delta k = 2.9$–10.1 Å^{-1}) of raw data minus calculated Ir–C, and Ir–O contributions (solid line) and calculated Ir-Si contribution (dotted line) characterizing the sample after 10 h of ethylene hydrogenation reaction under conditions stated in the text.
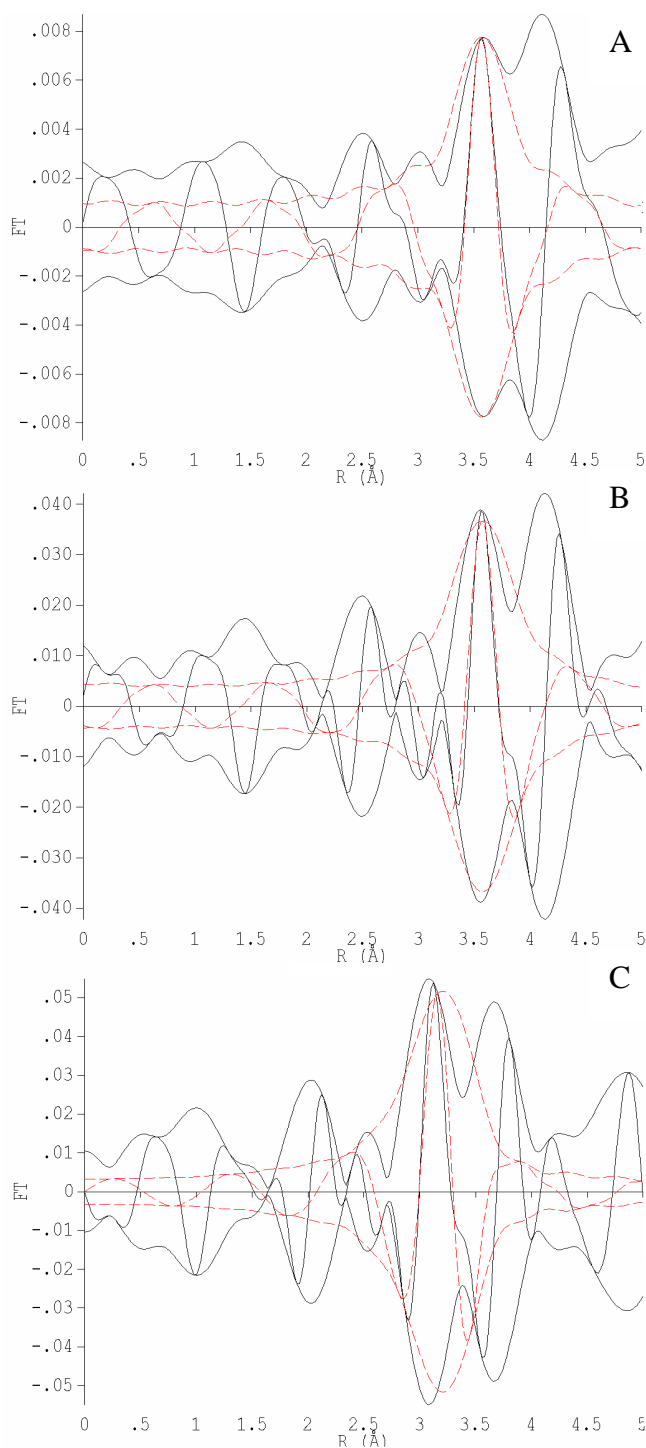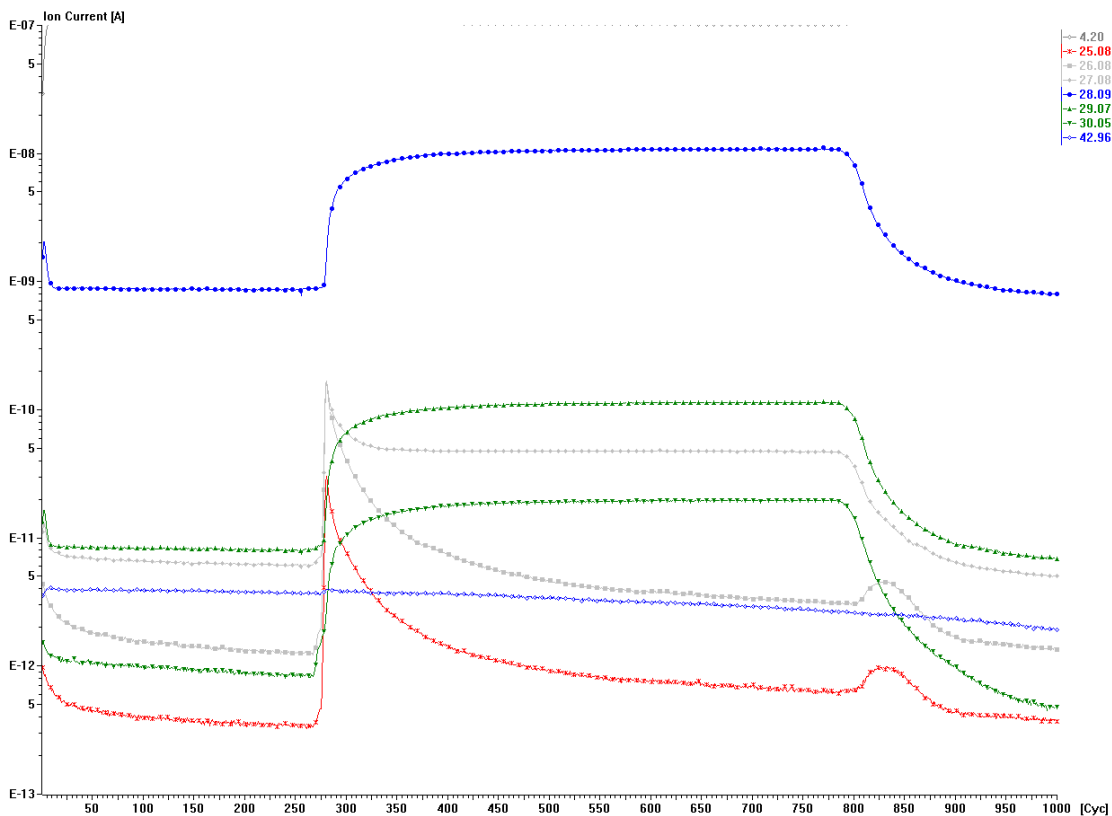
Figure SI-18. Mass spectra characterizing the outlet gas stream during CO treatment: exchange of ethylene ligands with CO and formation of gas-phase ethylene; *please see the following paragraph for the interpretation of the data.*

This graph represents the removal of the ethylene ligands following the introduction of CO to the IR cell containing the sample. One can expect the following masses for CO: m/z 28 and 29 (because of ^{13}CO with a natural abundance of 1.1%) and also m/z 30 (indicating the presence of $C^{18}O$ with a natural abundance of 0.21%). In Figure SI.18, the signals characterizing m/z 28, 29, and 30 follow a similar trend, and the intensity ratios of ion currents for these channels are in agreement with the abundance ratios of CO, ^{13}CO, and $C^{18}O$, respectively. Thus, we assign these m/z ratios to CO. On the other hand, m/z 25 and 26 are assigned as ethylene.

Additional information about Figure 8 (mass spectrometry results for the treatment of the as-prepared supported sample in H$_2$) from the main text:

Signals *m/z* = 25 and *m/z* = 30 during the treatment of the sample with H$_2$ are small, indicating that the rate of interaction of H$_2$ with the sample was very low. This slowness is related to the fact that most of the IR cell was not filled with solid sample and the treatment gas substantially bypassed the catalyst and therefore did not react with it. Thus, the time required for completion of this reaction was longer than allowed in the experiment. Therefore, the production of ethylene continued throughout the experiment.